INTERNATIONAL JOURNAL FOR NUMERICAL METHODS IN FLUIDS
Int. J. Numer. Meth. Fluids 2008; **56**:1233–1240
Published online in Wiley InterScience (www.interscience.wiley.com). DOI: 10.1002/fld.1746

A large eddy simulation of an airfoil turbulent wake subjected to streamwise curvature

E. Farsimadan and M. R. Mokhtarzadeh-Dehghan*, †

School of Engineering and Design, Brunel University, Uxbridge Middlesex UB8 3PH, U.K.

SUMMARY

This paper presents large eddy simulations (LES) of the curved wake of an airfoil. The wake was generated by placing a NACA0012 airfoil in a uniform stream of air, which is then subjected to an abrupt 90° curvature created by a duct bend. The trailing edge of the airfoil is one chord length upstream of the bend entry. The duct cross-section measures $457\,\text{mm} \times 457\,\text{mm}$, and the bend has radius to height ratio of 1.17. The flow Reynolds number (1.02×10^5) is based on a mainstream velocity of $10\,\text{m/s}$ and airfoil chord length 0.15 m. The sub-grid scale models employed are the classical Smagorinsky, its dynamic variant and the dynamic kinetic energy transport. The performance of LES in depicting the experimental flow is assessed and compared with results predicted by the Reynolds stress model (RSM). The results show the advantages of LES over Reynolds-averaged Navier–Stokes methods in predicting convex wall separation in strongly curved ducts on relatively coarse grids. Results from LES on a considerably finer near-wall-resolved grid lead to much improved comparison with the experimental data in the near wake, bettering predictions by RSM and LES on the coarse grid. Copyright © 2008 John Wiley & Sons, Ltd.

Received 22 March 2007; Revised 8 December 2007; Accepted 10 December 2007

KEY WORDS: LES; wake; airfoil; curvature; turbulent; duct

1. INTRODUCTION

Curved wakes occur in numerous industrial applications. Examples are in turbomachines, multi-element airfoils and ducts with guide vanes. It is known that curvature has significant effect on the properties of the wake. Experimental investigations of the curved wake of an airfoil [1] indicated enhancement of turbulence quantities on the inner-side wake and their suppression on the outer side. Steady-state Reynolds-averaged Navier–Stokes (RANS) computations [2] of the same flow field as in [1] with RSM qualitatively depicted the correct effects of curvature on

*Correspondence to: M. R. Mokhtarzadeh-Dehghan, School of Engineering and Design, Brunel University, Uxbridge Middlesex UB8 3PH, U.K.
†E-mail: reza.mokhtarzadeh@brunel.ac.uk

turbulence. However, clear discrepancies were evident in the quantitative comparison of wake profiles and in regions where separation occurred. A main source of discrepancy was a lack of prediction of separation on the convex wall of the 90° duct. The aim of the present work is to carry out large eddy simulations (LES) of the same flow in order to assess the ability of this technique in overcoming previous inaccuracies and to demonstrate the advantages it places over RANS methods. Several interesting features need to be examined; large vortical structures and their development in the near-wake, and flow separation on the convex wall. There have been a number of recent publications concerning LES of strongly curved duct flows, although to the best knowledge of the authors there exist no known publications on LES of curved wakes in the current configuration.

2. NUMERICAL METHOD AND COMPUTATIONAL SETUP

LES is a methodology developed from an understanding that the majority of energy is contained in the large scales of the flow. In LES, the Navier–Stokes equations are fully resolved for larger scales defined by the filter width, whereas the interactions of the resolved scales with the unresolved small scales are modelled using a sub-grid scale (SGS) model. The SGS models used in the present study are the classical Smagorinsky (SMG), its dynamic variant (DSMG) and the dynamic kinetic energy by transport (DKET). These models relate the eddy viscosity to the rates of strain through parameters C_s (SMG), c_s (DSMG) and C_k (DKET). In the SMG model C_s is fixed at 0.1. The parameters c_s and C_k are both dynamically determined, spatially at each point and temporally at each time step, thus providing better adaptation to local flow length scales. The DKET model differs from the DSMG model in that it additionally solves the turbulent kinetic energy transport equation to deduce k_{sgs} (SGS turbulent kinetic energy). Kim [3] provides further details of these models.

Wall functions defined by Werner and Wengle [4] have been adopted into the simulations. This consists of a two-layer approximation based on the viscous sub-layer and the assumption of a one-seventh power law outside the viscous sub-layer. The employed wall method presents advantages over standard wall function models by providing a more accurate representation of the near-wall layers. Mean velocity profiles measured upstream of the airfoil in [1] are used to define the inlet boundary conditions. The random flow generation technique in [5] based on samples of Fourier harmonics is used to generate a non-homogenous anisotropic flow field, representing turbulent inflow conditions. Within the implementation of this technique, the required turbulence quantities from the experimental data were used. The number of Fourier harmonics representing the turbulence spectrum is fixed at $N=50$. A fixed time step (seconds) $t=8.33\times10^{-3}c/U$ is chosen based on the mainstream velocity U and airfoil chord length c. Assessment of the Courant–Friedrichs–Lewy (CFL) number in the most turbulent regions indicated levels of CFL<1, confirming that the selected time step is capable of capturing the characteristic timescales of the flow. For the time integration an explicit four-stage Runge–Kutta scheme was used.

The majority of the simulations were conducted using the grid of [2], the results of which are referred to as coarseLES. This was in line with our initial aim to assess the degree of improvement, if any, which may be achieved using LES. This led to further simulations using a refined grid, the results of which are also included. The flow domain with the superimposed coarse grid is shown in Figure 1. The structured grid is composed of 25 blocks consisting of 676 000 cells, the full spanwise extent of the duct is represented by side walls, with 42 cells spaced evenly in the

DOI: 10.1002/fld

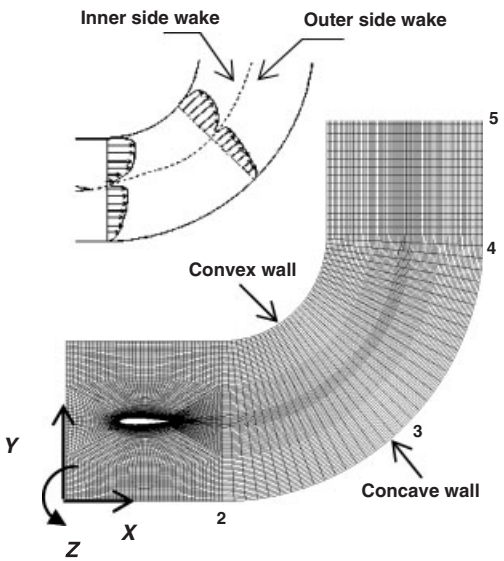

Figure 1. Computational coarse grid [2] and flow domain. Locations of stations 2–5 are indicated.

z-direction. A fine resolution was adopted close to the airfoil surface and the near-wake region. In non-dimensional wall units based on the local value of wall shear stress the near-wall airfoil grid spacings after $x/c=0.1$ are within $140>\Delta x^+>20$, $500>\Delta z^+>100$ and $\Delta y^+<1$ (wall to node distance for the first grid line). The coarse grid distribution in the normal direction on the bend walls ($\Delta y^+=100$) constitutes the reason behind adopting wall functions. The outlet is placed $5.0H$ downstream of station 4, where H is the cross-sectional duct height ($H=0.457$ m). In LES, the coarse spanwise resolution in the grid of [2] was considered to affect the boundary layer growth and the wake development. In response to this a refined grid was set up with a spanwise segment of the tunnel equal to $0.5c$, with periodic conditions defined in this direction. The refined grid has improved wall-normal, streamwise and spanwise resolutions throughout the domain consisting of more than 6.1 million cells and satisfies a near-wall resolution of $\Delta z^+<30$ over most of the airfoil.

The flow solver is based on the finite volume discretization of the governing equations. A bounded central differencing scheme is used to discretize the convection terms; this method is known to remove unphysical oscillations in the flow that are associated with pure central difference schemes, especially on coarser grids. The derivation of pressure is based on the SIMPLEC algorithm. Flow was allowed to develop for substantial computational time so that a statistically steady-state (SSS) condition for turbulence was achieved at station 5 (140 000 time steps or 50 flow through times). A further 40 000 time steps were computed with a sample taken every 10 time steps to obtain turbulence statistics. Simulations were carried out on a COMPUSYS parallel processing cluster. The grids were partitioned on 8 Intel Xeon dual processor nodes running at 3.2 GHz each. On the coarser grid this required an average of 3 s per time step, resulting in approximately 117 central processing unit (CPU) hours to reach SSS. Simulations on the finer grid took 12 s per time step with a running time of 470 CPU hours to reach SSS.

DOI: 10.1002/fld

3. RESULTS AND DISCUSSION

Figure 2 presents the measured and predicted pressure coefficient on the concave and convex walls of the duct. Pressures are relative to the reference value at station 1. There is general agreement between the experiment and the computation for the overall profile and also differences. On the convex wall, the predicted pressure drops to a minimum just before station 3 followed by a period of recovery leading to a distinct plateau. The plateau in the profile that is also seen experimentally was reported in [1] to be due to intermittent flow separation. This feature is not computed by RSM but predicted by coarseLES. However, the SMG model exaggerates this feature, whereas DSMG and DKET present better comparison to experiments. As stated before, the latter model uses an additional transport equation, which describes the physics of turbulence better and provides improved results compared with DSMG. LES also shows closer agreement for the pressure recovery downstream of station 4 and also for the overall pressure loss.

On the concave wall, between stations 1 and 2, coarseLES predicts a small plateau in the pressure profile (Figure 2), a feature not computed in RSM or measured in the experiment. This can be attributed to the occurrence of small flow separation upstream of station 2 as can be seen in Figure 3(a), where the velocity vector field at the midspan is shown. This is believed to be due to the jump in the streamwise grid resolution in this region. In Figure 3(b) the velocity vectors indicate separation from the convex wall just before station 4, where flow is reversed in the vicinity close to the wall. Reattachment is observed at a distance less than the duct height H, downstream of the separation point.

Profiles of streamwise velocity, turbulence intensity and turbulence shear stress at station 5 are presented in Figure 4(a)–(c). LES has computed the velocity and turbulence fields near the convex wall in very good agreement with experiments. All SGS models perform consistently well in this respect. The enhancement of turbulence is attributed to the separation and recirculation resolved by LES, observed in Figure 3(b). Lack of prediction of flow separation on the convex wall by RANS is evident by very low levels of turbulence demonstrated in Figure 4(b). The wake velocity defect and turbulence profiles as predicted by RANS and experiments have reduced considerably

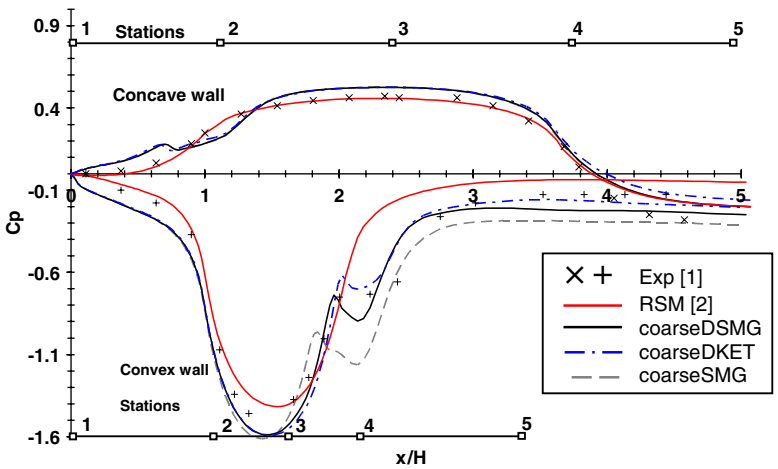

Figure 2. Pressure coefficient along the convex and concave walls of the duct.

DOI: 10.1002/fld

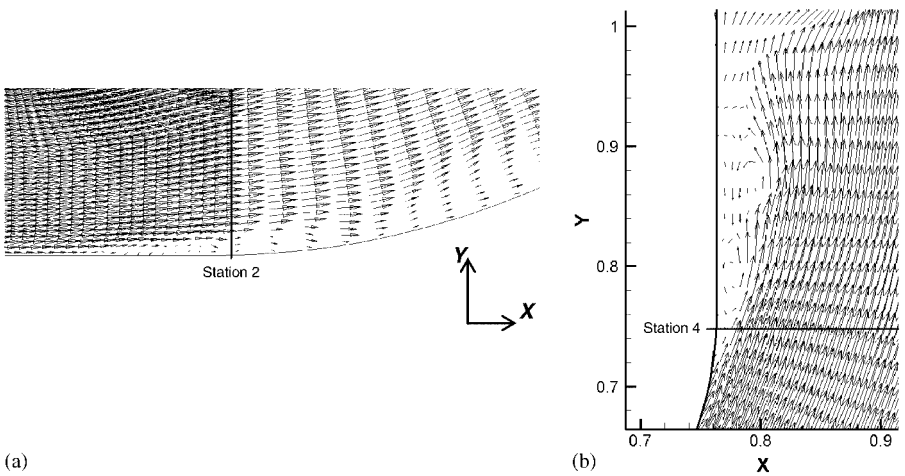

Figure 3. Velocity magnitude vectors plotted midspanfor coarseDSMG: (a) near the concave curvature at station 2 and (b) at the convex wall past station 4.

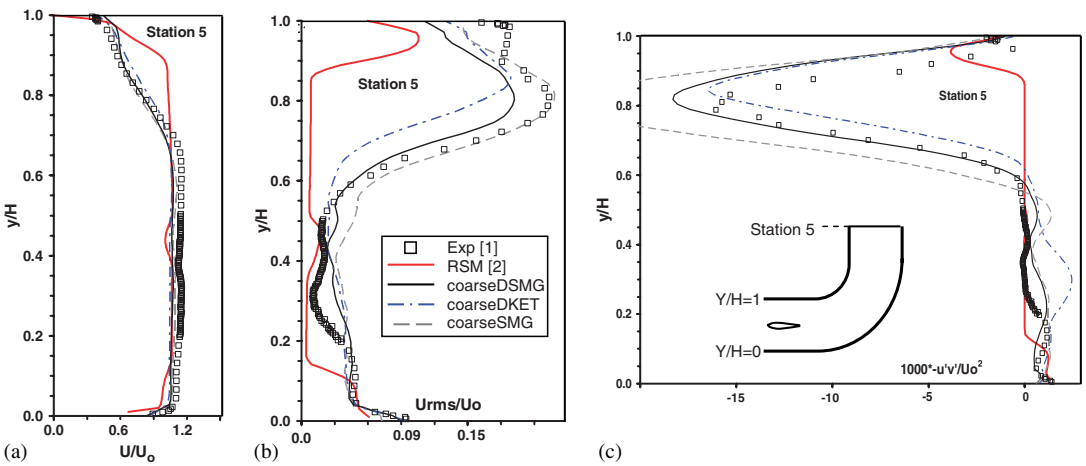

Figure 4. Mean velocity and turbulence quantities predicted by coarseLES across full duct height at station 5: (a) streamwise velocity; (b) streamwise turbulence intensity; and (c) turbulence shear stress.

in magnitude by station 5. In the coarseLES the wake has washed out in this region with less distinguishable features. The results in the highly separated region demonstrate the advantages of LES over RANS in this strongly curved convex curvature.

Figure 5(a), (b) illustrates a comparison of mean streamwise velocity and turbulence intensity in the near wake for $x/c = 1.326$, 1.443 and 2. This figure also presents new experimental data in the wake. The previous studies [1, 2] showed that, relative to the duct centreline, the wake is shifted towards the convex wall at stations 2 and 3, and then towards the concave wall at stations 4 and 5. This was confirmed by the present simulations. In comparison to RSM, coarseLES resolves an

DOI: 10.1002/fld

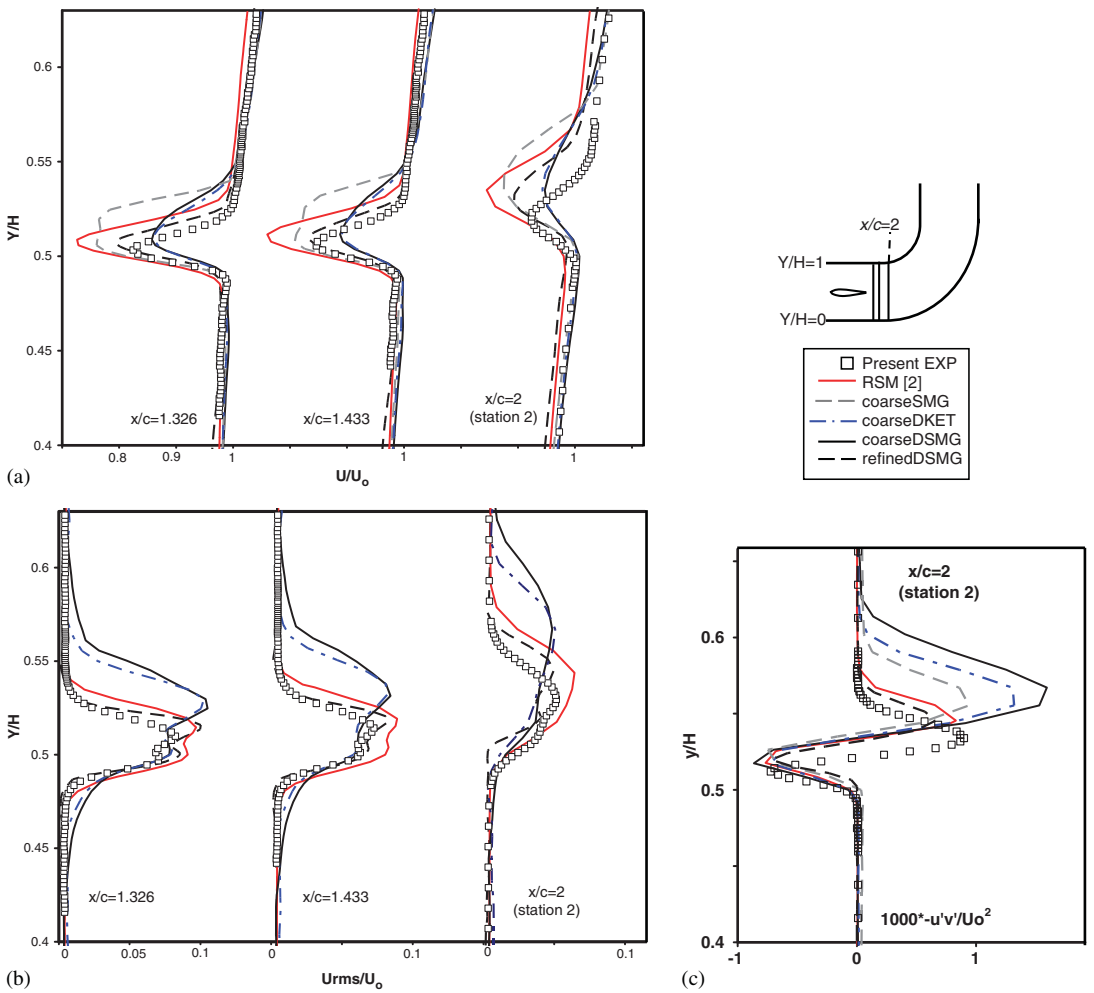

Figure 5. Comparison between coarseLES on the grid of [2] and preliminary results of LES on a refined grid: (a) mean streamwise velocity; (b) streamwise turbulence intensity; and (c) turbulence shear stress.

increased wake width at station 2, a feature that is consistent throughout the downstream stations. CoarseSMG predicts a considerably enhanced profile on the inner side of the wake with larger velocity defect. The dynamic models on the same grid compute a smaller velocity defect. In all computations the centre of the wake is located above the experimental profile. The SMG model resulted in an erroneous streamwise turbulence intensity profile in the wake, results of which are omitted. In Figure 5(b) in comparison to RSM the existence of a double peak in the profile is better depicted by the simulations, but the turbulence intensity is considerably overpredicted on the inner side for the dynamic SGS models in coarseLES. This is believed to stem from the overprediction of turbulence on the upper surface of the airfoil, which was also stated in [2]. The results indicate that the boundary layer predictions on the airfoil have worsened in the case of coarseLES leading

DOI: 10.1002/fld

to larger differences in the curved wake. These differences remain in the profiles at downstream stations 3 and 4 (not shown here). Turbulence shear stress at station 2 in Figure 5(c) is enhanced on the inner side of the wake and suppressed on the outer side. Although this is qualitatively correct, the level of turbulence enhancement in coarseLES is computed too high when compared with RANS and experiments.

In light of the shortcomings of LES on the grid of [2], in the wake, results for the refined grid of reduced spanwise extent are also presented in Figure 5. Results from refinedDSMG indicate vast improvements in the prediction of the wake properties. The wake defect, wake width and, in particular, the presence of a double peak structure in the turbulence intensity profiles are in close agreement with the experiments, surpassing the RSM predictions in Figure 5(b) and (c). We have not included the results for stations 3 and 4, but the improvements noted here remain consistent. Despite the improvements noted in the wake, the results also showed deterioration by predicting a smaller separation region on the convex wall. This is due to the shortened spanwise extent of the flow domain, and in place of the side wall, the imposition of the periodic condition. The inaccurate prediction of the location of the wake centre (Figure 5(a)) still remains consistent with RANS and coarseLES especially at $x/c=2$ when the effect of curvature is more pronounced. This points to a need for further investigations.

Figure 6(a)–(c) presents contours of spanwise vorticity in the near wake as computed by coarseSMG, coarseDSMG and refinedDSMG, respectively. The merging shear layers on the upper and lower surfaces of the airfoil have resulted in the formation of counter rotating vortices in the wake. The effects of curvature on the inner side of the wake compared with the outer side are evident in this figure. As with the velocity and turbulence profiles, the near-wake vorticity is also shifted above the duct centreline. Results from coarseSMG (Figure 6(a)) present a somewhat different pattern compared with the pattern of coarseDSMG (Figure 6(b)), where the latter provides more plausible representation of the dynamic vortical structures on the coarse grid. This is considered to be in response to the limitations of the standard SMG model in representing the local length scale. Results from the classical LES case described by refinedDSMG (Figure 6(c)) indicate a highly resolved vorticity field near the trailing edge, which is in direct response to the increased spanwise, wall-normal and streamwise grid resolutions in the region of the airfoil. The vortex pattern observed in Figure 6(c) on the upper surface of the airfoil near the trailing edge indicates

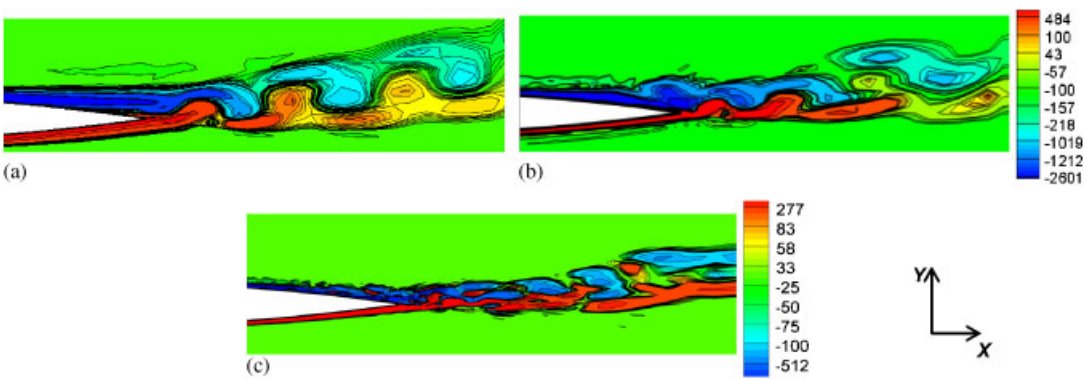

Figure 6. Development of spanwise vorticity (ω_z) in the near wake: (a) coarseSMG; (b) coarseDSMG; and (c) refinedDSMG on the refined grid.

DOI: 10.1002/fld

features of transitional flow, the correct prediction of which is important in resolving the developing wake downstream.

4. CONCLUSIONS

On the coarse grid, LES displayed advantages over RANS in predicting flow behaviour near strong convex curvature, but also shortcomings in relation to the prediction of wake parameters. The dynamic variants of the SGS models were more accurate in predicting flow near the trailing edge and in the wake of the airfoil. The better prediction of wake parameters on the refined grid is due to the improved simulation of the boundary layers on the upper and lower surfaces of the airfoil, as a result of improved grid resolution. The effect of curvature, that is, the increase in turbulence on the convex side of the wake and the decrease in the concave side, and the existence of a double peak in the profile was better predicted by refinedLES. Quantitative differences between refined LES and experiments relate in particular to the inaccurate prediction of the location of wake centre, which needs to be investigated further.

ACKNOWLEDGEMENTS

The study was carried out with FLUENT 6.3.21. Post-processing was conducted with TECPLOT 360.

REFERENCES

1. Piradeepan N, Mokhtarzadeh-Dehghan MR. Measurements of mean and turbulence quantities in the curved wake of an airfoil. *Experimental Thermal and Fluid Science* 2005; **29**:239–252.
2. Mokhtarzadeh-Dehghan MR, Piradeepan N. Numerical prediction of a turbulent curved wake and comparison with experimental data. *International Journal for Numerical Methods in Fluids* 2006; **51**:49–76.
3. Kim S. Large-eddy simulation using an unstructured mesh based finite-volume solver. *Technical Report AIAA-2004-2548*, *American Institute of Aeronautics and Astronautics*, *34th Fluid Dynamics Conference and Exhibit*, Portland, Oregon, 2004.
4. Werner W, Wengle H. Large-eddy simulation of turbulent flow over and around a cube in a plate channel. *Eighth Symposium on Turbulent Shear Flows*, Munich, Germany, 9–11 September 1991; 155–168.
5. Smirnov A, Shi S, Celik I. Random flow generation technique for large-eddy simulations and particle-dynamics modelling. *Journal of Fluids Engineering* 2001; **123**:359–371.

DOI: 10.1002/fld